JOURNAL OF APPLIED ELECTROCHEMISTRY **29** (1999) 347–353.

Corrosion and corrosion inhibition of nickel in $HClO_4$ solutions using the EQCM technique

F. ZUCCHI, M. FONSATI, G. TRABANELLI

Corrosion Study Centre "A. Daccò", Department of Chemistry, University of Ferrara I-44100 Ferrara, Italy

Received 23 December 1996; revised 18 April 1997

Application of the electrochemical quartz crystal microbalance (EQCM) to the study of metal corrosion and its inhibition is rather recent. Among the advantages of this technique are its very high sensitivity and the possibility of simultaneous mass variations and voltammogram recording. These characteristics suggest the use of the EQCM for research in very low corrosion rate conditions. This paper reports the results of EQCM measurements on the corrosion inhibition rates of Ni in 0.1 M $HClO_4$, in the absence and presence of different inhibitors in free corrosion conditions, for following inhibitors: acridine (A), benzyl quinolinium chloride (BQCl), dodecyl quinolinium bromide (DDQBr), tributylbenzyl ammonium iodide (TBNI) and potassium iodide (KI). The corrosion rate was reduced considerably by KI and TBNI. DDQBr showed a good inhibitive efficiency, while BQCl had only a small effect, and A stimulated corrosion of the Ni. Voltammograms at different scanning rates and the mass variation in the same solutions were recorded. Comparison of the current density and the mass changes provided the basis for a qualitative interpretation of the passivation of Ni and the mechanism of action of the different inhibitors.

Keywords: *corrosion inhibition*, *metal corrosion*, *quartz crystal microbalance*

1. Introduction

The electrochemical quartz crystal microbalance (EQCM) has only recently found application in the study and monitoring of corrosion [1] and corrosion inhibition [2] phenomena. Due to the very high sensitivity of this technique, literature data deal with systems showing low corrosion rates, such as copper in neutral aqueous solutions [2–4].

The possibilities of recording simultaneously the mass variations of the metal electrode and the corresponding voltammogram [5] or the EIS spectrum [6] have contributed to the wide number of applications of the EQCM technique. The present paper reports experimental results for the corrosion of nickel in 0.1 M $HClO_4$ solutions in the absence and presence of various inhibitors.

2. Experimental details

A Seiko/EG&G EQCM (model QCM917) was used, connected to a EG&G (model 273) potentiostat. The oscillators were quartz crystals, having the characteristics shown in Table 1. A Ni layer was electroplated on the gold surface using a current of 24 mA for 30 s from a Watts bath.

The 0.1 M $HClO_4$ solutions were prepared from pure reagent and distilled water. The solutions were used without previous deaeration. The following compounds, pure reagent grade, were tested as inhibitors, at 10^{-3} M concentration: acridine (A), benzyl quinolinium chloride (BQCl), dodecyl quinolinium bromide (DDQBr), tributylbenzyl ammonium iodide (TBNI) and potassium iodide (KI).

All tests were conducted at 25 ± 0.1 °C in a double wall Pyrex cell previously described [4]. Corrosion tests were conducted on nickel electrodes at free corrosion potential, with simultaneous recording of the frequency as a function of time. Voltammograms were recorded starting from the free corrosion potential value up to +1000 mV vs SCE, with scanning rates from 10 to 50 mV s^{-1}. A Nicolet spectrometer (model Magna-IR 550), equipped with FT-80, was used to record the FTIR reflection spectra on nickel sheets, after 24 h immersion in solutions of the various inhibitors. All the potentials quoted in the text are referred to the saturated calomel electrode (SCE).

3. Results

3.1. *Tests in free corrosion conditions*

Figure 1 collects the mass variation/time curves of Ni in 0.1 M $HClO_4$ solutions in the absence and presence of the various additives. It is clearly shown that the mass variations in 0.1 M $HClO_4$ are almost linear.

Acridine shows two different trends: initially very low mass variations of nickel were recorded, whereas with increasing time, the decrease in mass of the electrodes was higher than that corresponding to the blank tests. In conclusion, acridine exerts a stimulating effect (I.E. = −53% where I.E. is inhibiting efficiency, the negative implying an accelerating effect on corrosion rate) on the corrosion of nickel in the

Table 1. Characteristics of the EQCM

Resonant frequency	9 MHz
Cut type	AT cut
Electrode material	sputtered Au on a Ti substrate
Electrode area	$\sim 0.2\,cm^2$
Electrode diameter	5 mm
Electrode thickness	Au approx. 300 nm, Ti approx. 50 nm
Mass	~ 0.3 g

experimental conditions adopted. BQCl was found to be quite ineffective (I.E. = 14%), whereas the behaviour of DDQBr can be considered satisfactory (I.E. = 84%). Inhibiting efficiencies of about 100% were found for Ni in the presence of KI and TBNI.

Figure 2 shows the trends of the mass changes of nickel electrodes with time in 0.1 M $HClO_4$ solutions, in which various inhibitors were added only 30 min after immersion of the metal electrodes. The inhibitor concentration was 10^{-3} M. The stimulating effect of A, the negligible effect of BQCl and the good efficiency of DDQBr previously described are confirmed. In the presence of TBNI and KI the corrosion rate is completely blocked; no further mass changes were measured.

Figure 3 collects the potential variations measured on nickel electrodes in 0.1 M $HClO_4$ in the presence of the various additives, under the experimental conditions described in Fig. 2. The potential change provoked by addition of A is negligible. A gradual shift of about 100 mV towards more noble potentials is promoted by the introduction of BQCl. A positive jump of about 170 mV occurs just a few minutes after the addition of DDQBr. Very high (200–250 mV) and instantaneous potential shifts of nickel electrodes are provoked by the addition of TBNI or KI to the $HClO_4$ solutions. Comparison of Figs 2 and 3 show the influence of time on the interaction between the different inhibitors and the metal surface. The adsorption of TBNI and KI is almost instantaneous with consequent blocking of the corrosion process, whereas the adsorption of the other additives requires a definite time.

3.2. *Cyclic voltammetry*

Figure 4 shows the voltammogram recorded with the EQCM on Ni in 0.1 M $HClO_4$ in the interval from the corrosion potential up to +1000 mV at a scan rate of $50\,mV\,s^{-1}$. A first anodic peak is clearly evident followed by a lower second peak, after which the passive current diminishes until +1000 mV. The current during the reverse scan continues to remain very low. This suggests that the passive film is not reduced during the reverse scan.

Figure 5 shows the corresponding mass variations of the nickel electrode. At the beginning of the anodic curve a small weight increase occurs. This increase is then followed by continuous weight loss of the electrode up to the end of the first current peak. The initial increase in mass ($\Delta m = 0.3\,\mu g\,cm^{-2}$) can be related to the surface adsorption of OH^- ions; indeed, this has been suggested [7] as the first step of the anodic dissolution of Ni. The Δm value of $0.3\,\mu g\,cm^{-2}$ corresponds to the formation of about 16 OH^- layers at the surface. Bourkane *et al.* [8] assumed a roughness factor of 10 for Au sputtered on quartz and a further increase in the roughness factor (about 1.5 times) can be assumed for nickel plated on Au. On this basis the formation of a OH^- monolayer can be calculated. In correspondence to the second current peak, the slope of the $\Delta m/E$ curve is much lower, and the mass of the electrode remains quite constant until +1000 mV. On the reverse curve,

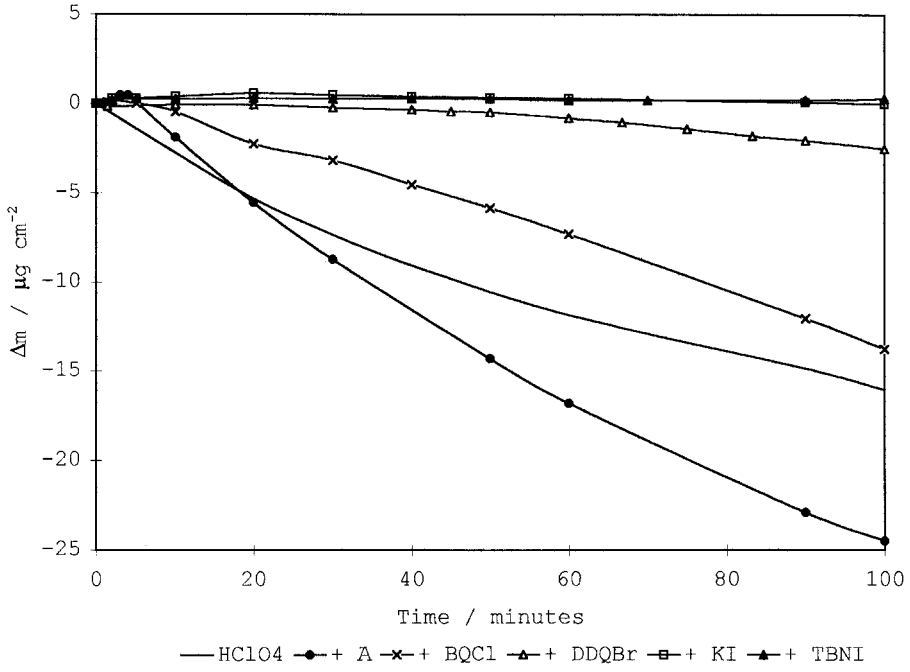

Fig. 1. Mass variations against time curves of Ni in 0.1 M $HClO_4$ solutions in the absence and presence of corrosion inhibitors.

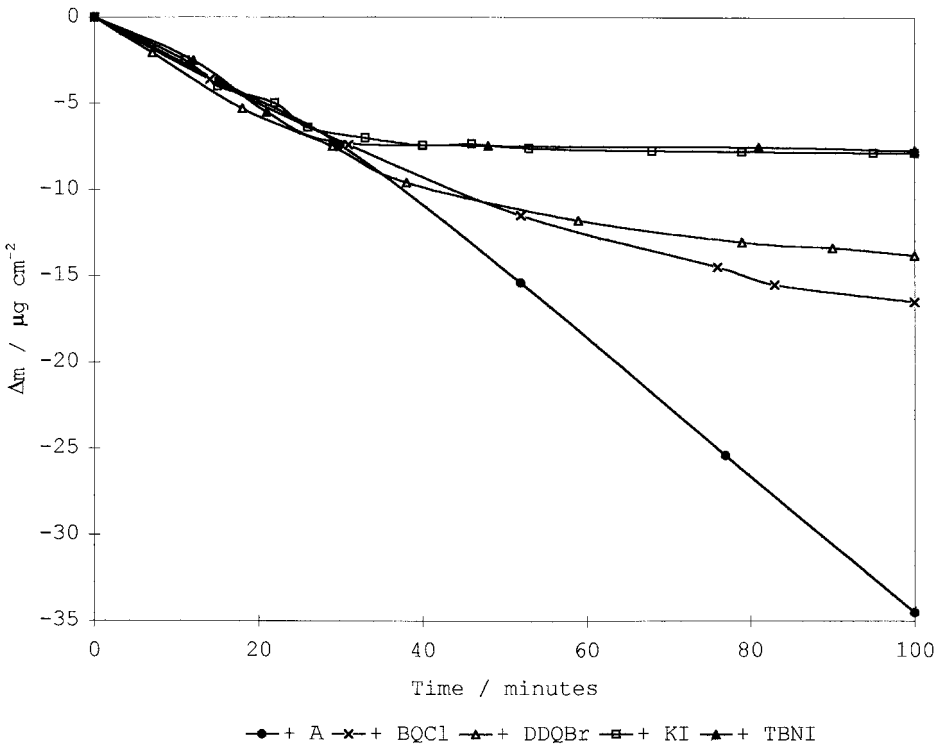

Fig. 2. Mass variations against time of Ni in 0.1 M $HClO_4$ solutions. Inhibitors added after 30 min.

almost negligible mass variations of the nickel electrode occur. These curves agree with the passivation mechanism suggested by De Gromoboy [7] for nickel. As mentioned above, the first step is attributed to the formation of the unstable adsorbed intermediate according to the following equation:

$$Ni + OH^- \longrightarrow NiOH_{ads} + e^-$$

This intermediate can further react in two different ways. On the one hand, oxidation and protonation of the intermediate to Ni^{2+}, unable to passivate the metal, leads to the active corrosion of Ni according to the following equation:

$$NiOH_{ads} + H^+ \longrightarrow Ni^{2+} + e^- + H_2O$$

On the other hand, oxidation and deprotonation of the same intermediate leads directly to passivation according to the equation:

$$NiOH_{ads} \longrightarrow NiO + H^+ + e^-$$

The surface NiO film constitutes only the first step in Ni passivation. With polarization of the electrode

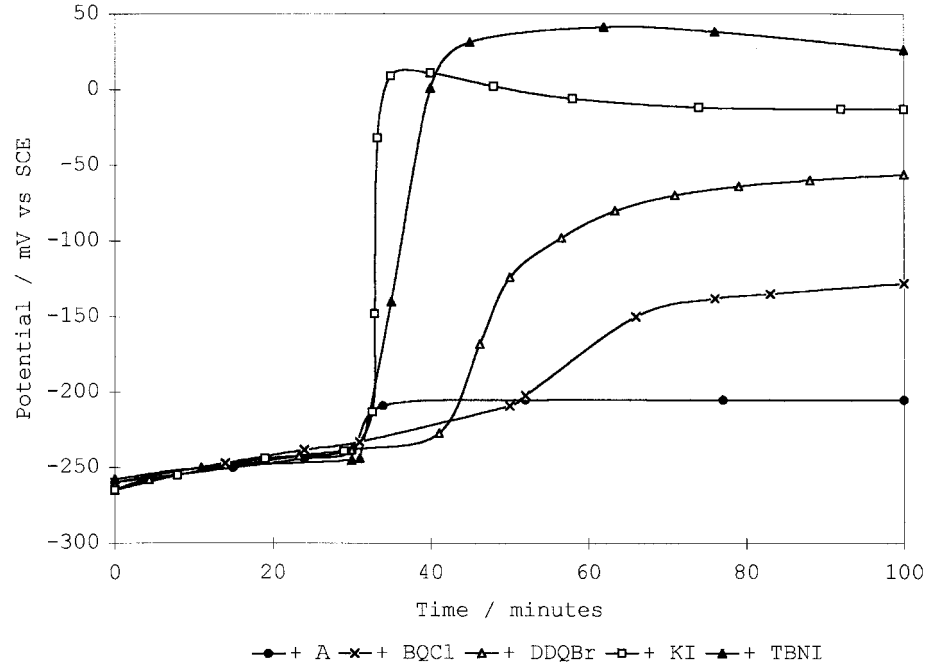

Fig. 3. Potential variations of Ni in 0.1 M $HClO_4$ solutions. Inhibitors added after 30 min.

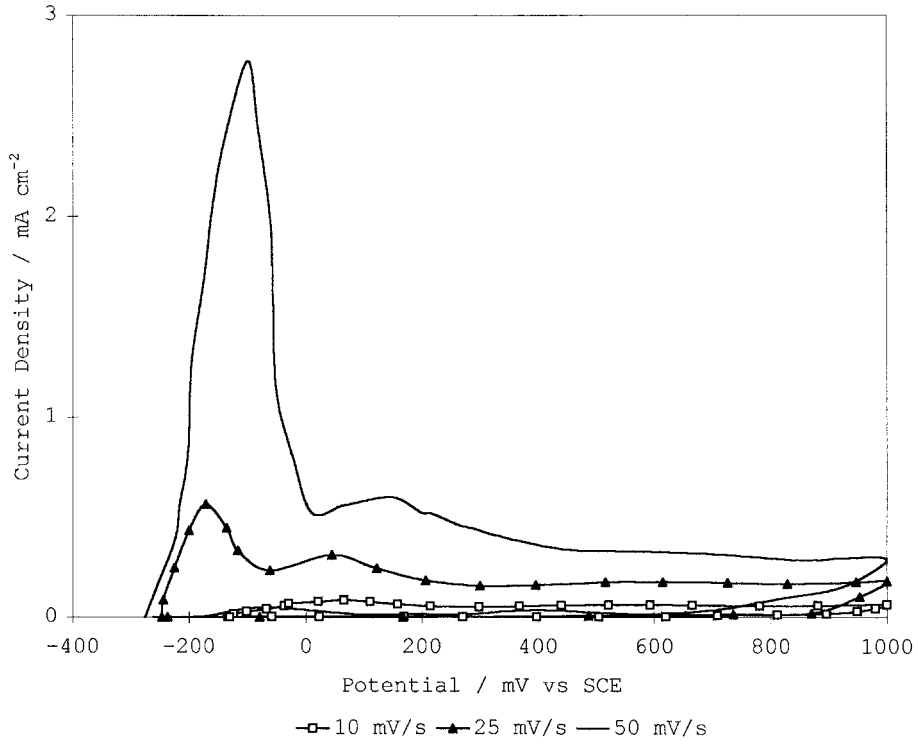

Fig. 4. Voltammograms recorded by EQCM on Ni in 0.1 M $HClO_4$ solutions with various scanning rates.

towards more positive potential values, higher oxides of Ni can be formed once the equilibrium potential values are exceeded. The presence of NiO_x imparts stable passivity to the metal [7].

The first current peak reported in Fig. 4 can be attributed to NiO, whereas the second peak is related to the formation of higher nickel oxides. By comparing the potential of the second peak with the thermodynamic values characteristic for the formation of various higher nickel oxides, the NiO_x formed can be identified as Ni_2O_3.

Figure 4 also reports the voltammograms recorded at different scan rates: 50, 25 and 10 $mV\,s^{-1}$. The decrease in scan rate leads to a decrease in the current density corresponding to the first peak, whereas the second peak continues to remain definite. This behaviour can be related to the passivation mechanism of nickel. The lower the rate of polarization, the

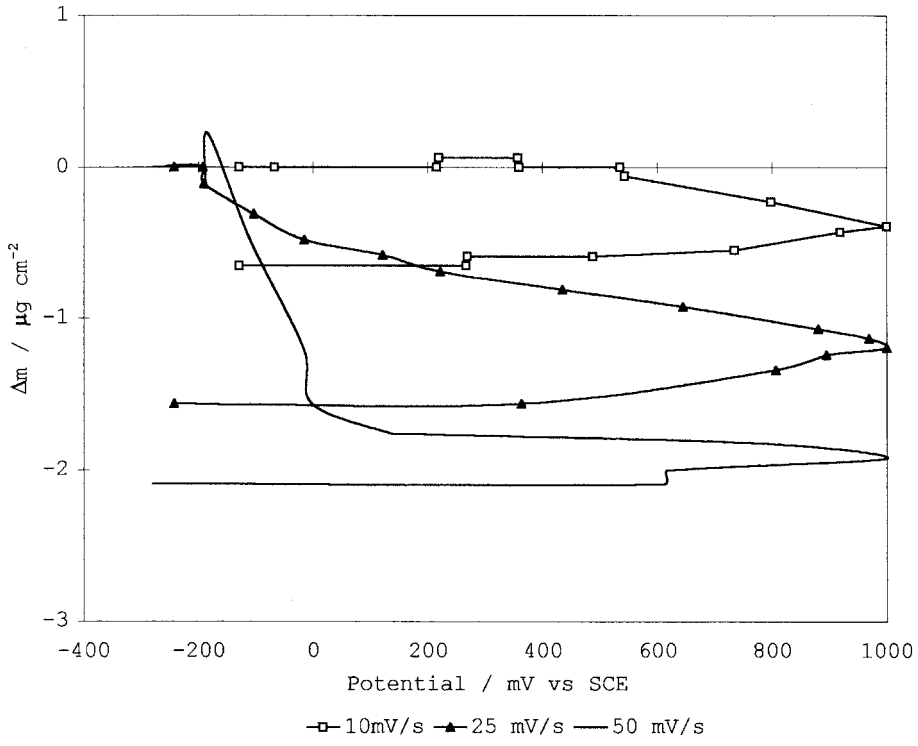

Fig. 5. Mass variations of Ni against potential, during the recording of the voltammograms of Fig. 4.

easier the formation of NiO. For this reason the current of the first peak is lower, whereas the shape of the second peak, as mentioned above, is also clearly defined at lower scan rates. Figure 5 shows mass variations measured on the nickel electrodes during polarization in the three selected conditions. The whole mass changes are influenced considerably by the scan rate. At a scan rate of 50 mV s^{-1} a decrease in mass of about 2.1 $\mu g\,cm^{-2}$ is found which decreases further to 1.5 $\mu g\,cm^{-2}$ at 25 mV s^{-1} and 0.6 $\mu g\,cm^{-2}$ at 10 mV s^{-1}. The trends of the mass variations corresponding to the various scanning rates are clearly different in shape and slope. The values of the mass variations agree with the anodic charge quantities (Q_a) calculated from the voltammograms passing from 17 to 12 and 7 mC cm^{-2} as the scanning rate decreases from 50 to 25 and 10 mV s^{-1}, respectively. In all cases, the weight decreases recorded by the microbalance are lower than the corresponding values calculated from (Q_a), the anodic charge amounts.

3.3. *Voltammograms recorded in the presence of inhibitors*

Figure 6 shows voltammograms recorded in the presence of the various compounds, starting from the corrosion potential up to +1000 mV. All the compounds examined shift the corrosion potential in the positive direction. E_{corr} values increase in the order:

$$A < BQCl < DDQBr < TBNI = KI$$

following the sequence of the inhibiting efficiencies of the compounds. All the anodic curves show a first peak in which the current values decrease, passing from A, BQCl, DDQBr to TBNI and KI. The value of the peak potential shifts from −100 mV in the presence of A to +300 mV in the presence of TBNI and KI. A second peak is evident at +530 mV for KI, at +670 mV in the presence of DDQBr and at +550 mV in the presence of BQCl.

The nature of this second peak can be attributed to various factors, such as: (i) oxidation of the halides at the electrode; (ii) oxidation of the organic cations, in the cases of BQCl and DDQBr; and (iii) interaction of the halide anions with the passive layer.

Voltammograms recorded on Pt electrodes in the above mentioned potential interval showed that only when working in KI solutions could the iodide ion be oxidized to iodine at a potential value around +500 mV. In contrast, in the presence of organic additives containing halides, no oxidation peaks were found. For this reason, it is assumed that the anodic polarization of nickel produces desorption of the inhibitor at more noble potentials as the adsorption of the halide ion ($Cl^- < Br^- < I^-$) increases and the first oxidation peak appears with formation of the passive film. I^- ions can be oxidized on this layer. When Cl^- or Br^- ions are present, they tend to attack the passive film, giving rise to the second peak, which is clearly higher in the presence of chlorides than in the presence of bromides.

By comparison, some voltammograms were recorded with the EQCM in solutions containing 10^{-3} M concentrations of KCl and KBr. The characteristic peaks found in the presence of halide containing inhibitors were recorded at the same potentials, but with higher current density. The mass

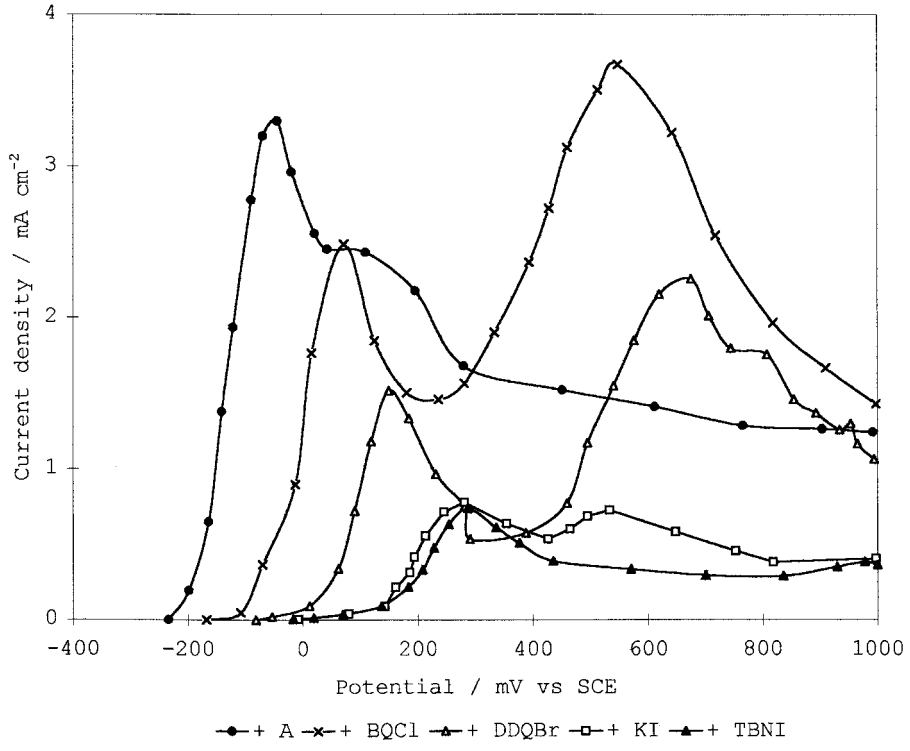

Fig. 6. Voltammograms recorded by EQCM on Ni in 0.1 M $HClO_4$ solutions in the presence of the corrosion inhibitors.

variations are similar, but greater than in the presence of the organic cations.

The decrease in current after the second peak can be attributed to repassivation of pits as Vetter and Strehblow [9] showed on iron. Actually, these authors found that pits on iron in solutions containing halides and ClO_4^- were active only in a potential range between $\varepsilon_L < \varepsilon < \varepsilon_I$. At potential values higher than ε_I, the pits were repassivated. The ε_I value depends only on the ratio of the concentration of the anions.

Analysis of the mass change curves confirms the above mentioned hypotheses. In fact, it is shown that the total mass changes recorded during the cyclic voltammetric tests can be correlated with the inhibiting efficiencies of the various additives.

The mass changes of the electrode recorded in the presence of A (Fig. 7) present a shape very similar to that recorded in the blank test. The higher current values shown in the potential range from 0 to +1000 mV on the voltammogram recorded in the presence of A, are attributed to the continuous decrease in mass related to the hindering of formation of a stable passive film.

In the presence of BQCl (Fig. 7) the mass of the electrode remains constant from E_{corr} to about 0 mV, then decreases in correspondence with the first current peak value. Successively, the mass remains constant until a sudden decrease occurs corresponding to the second current peak. The stability of the mass in the first zone of the anodic curve can be attributed to the 'zero' difference between the formation of solid surface products (Ni oxides) and the dissolution of the metal. The first mass decrease is the result of desorption of the inhibitor, partial dissolution of nickel and formation of the passive layer. The second decrease in mass can be attributed to partial destruction of the oxide film due to the aggressivity of the chloride ions. A curve of the mass changes similar to that corresponding to BQCl was recorded in the presence of DDQBr (Fig. 7). Also in this case two zones of mass changes are found; the first related to formation of the passive layer and the second related to the action of the bromide ion. The total decrease in mass is lower in the presence of DDQBr, confirming that Br^- is less aggressive than Cl^-.

In the presence of KI (Fig. 7) the mass of the electrode remains fairly constant until the end of the second current peak at about +500 mV. The position of the corrosion potential near 0 mV suggests that the low anodic current recorded is related to the direct formation of the passivating NiO_x. The mass of this nickel oxide should compensate for the desorption of iodide and residual dissolution of the nickel, negligible due to the action of KI. The increase in mass corresponding to more noble potentials can be related to the adsorption of iodine on the oxide surface. Indeed an increase in mass was found corresponding to the second current peak, where the presence of the oxidation reaction of iodide to iodine was demonstrated.

The voltammograms recorded from E_{corr} to +1000 mV in the presence of TBNI are similar to those shown in solutions containing KI (Fig. 6). The quantity of anodic charge is slightly lower in the case of TBNI. The trend of the mass variations recorded in the presence of TBNI is similar to that corresponding to KI (Fig. 7). The mass changes of the electrodes are very low until near +1000 mV, whereas during the not reported reverse sweep an increase in mass occurs up to +500 mV, after which the mass remains constant. This increase in mass can be

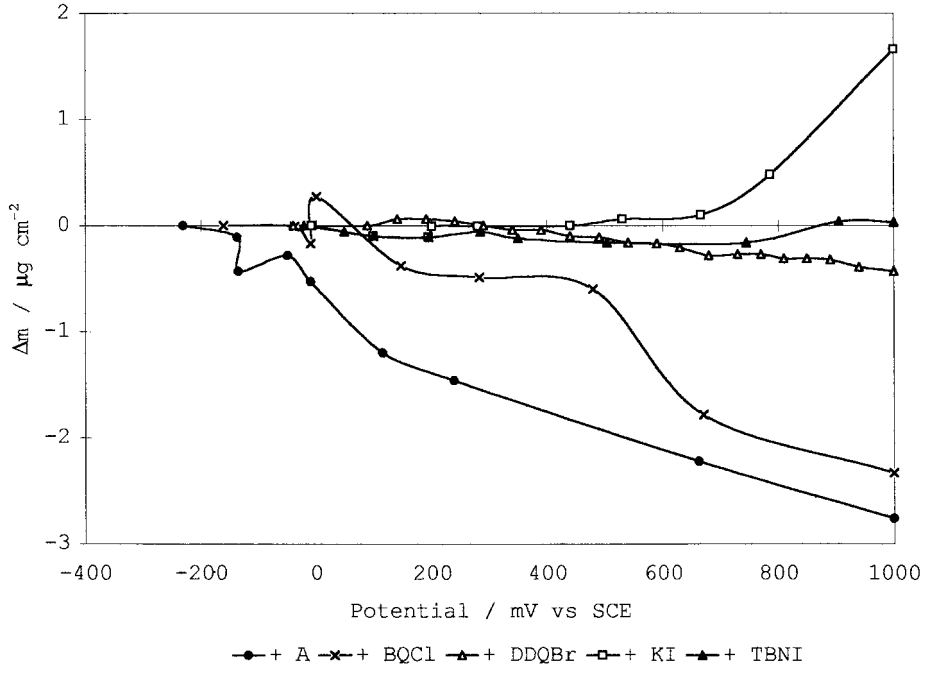

Fig. 7. Mass variations of Ni against potential during the recording of the voltammograms of Fig. 6.

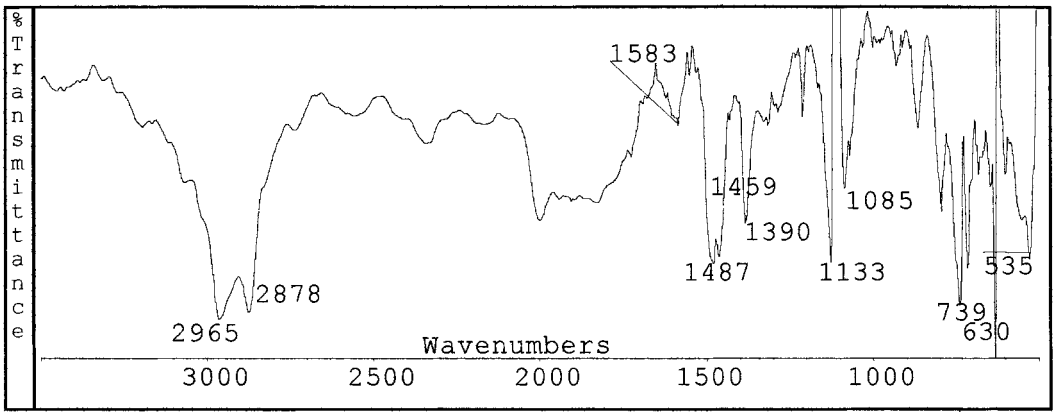

Fig. 8. FTIR reflection spectrum recorded on Ni sheets after 24 h immersion in 0.1 M $HClO_4$ solution in presence of TBNI.

explained as in the presence of KI, assuming the adsorption of iodine on the passive layer.

3.4. *FTIR measurements*

The FTIR reflection spectra were recorded on Ni sheets after immersion in $HClO_4$ solutions, containing some of the most efficient inhibitors, such as BQCl, DDQBr and TBNI.

Figure 8 reports, as an example, the FTIR spectrum recorded on Ni in the presence of TBNI. The presence of the inhibitor at the surface is confirmed by the characteristic bands of benzene: (i) C=C stretching (1583–1487 cm^{-1}); (ii) ring stretching (1085 cm^{-1}); and (iii) C—H bending (739 cm^{-1}). The bands of the aliphatic chain are also present: (iv) C—H stretching of the CH_3 group (2965 cm^{-1}); (v) C—H stretching of the CH_2 group (2878 cm^{-1}); (vi) C—C stretching (1133 cm^{-1}); and (vii) C—C rocking (535 cm^{-1}).

A comparison between the infrared spectra of the pure compounds tested as inhibitors and the reflection spectra recorded after immersion of the metal sheets in acid solutions of the inhibitors does not show any variation in the molecular structure. Therefore, it can be assumed that initially the inhibitors are physically adsorbed on the metal surface. The spectra recorded after successive rinsing of the metal sheets with distilled water show the permanence of the organic inhibitors on the metal surface. This behaviour appears to confirm a chemisorption process through the π electrons of the aromatic part of the molecule.

4. Conclusions

Results obtained with the EQCM shows that this technique can give a valuable contribution to the interpretation of corrosion and corrosion inhibition mechanisms. The responses obtained by the microbalance must be interpreted, however, as the result of a number of factors.

In the absence of inhibitors, the response of the EQCM in tests conducted at free corrosion potential can be considered univocal, since the formation of solid surface corrosion products is impossible at the pH selected for the experiments. Thus, the response of the EQCM permits determination of the dissolution kinetics of the electrode and calculation of its corrosion rate.

In the presence of inhibitors the variation in mass must be considered as the difference between the formation of a surface layer $(+\Delta m)$ and the dissolution of the metal $(-\Delta m)$. The inhibitors studied can adsorb on the surface of the metal, hindering the anodic dissolution as a function of their molecular characterisitics. The voltammograms showed a relationship between the ennoblement of the corrosion potential, the variations in mass and the inhibiting efficiency of the various compounds tested.

Acknowledgement

This work was (60%) financially supported by the MURST fund.

References

[1] S. P. Sharma, *J. Electrochem. Soc.* **127** (1980) 21.
[2] D. Jope, J. Sell, H. W. Pickering and K. G. Weil, *J. Electrochem. Soc.* **142** (1995) 2170.
[3] A. Shaban, E. Kálmán and J. Bácskai, Proceedings of the 8th European Symposium on 'Corrosion Inhibitors', Ann. Univ. Ferrara, N. S., Sez.V, suppl. 10 (1995), p. 951.
[4] F. Zucchi, M. Fonsati e G. Trabanelli, 'Giornate Nazionali sulla Corrosione e Protezione – 3° Edizione', AIM, Milano (1996), p. 115.
[5] D. Kouznetsov, A. Sugier, F. Ropital and C. Fiaud, *Electrochim. Acta* **40** (1995) 1513.
[6] O. Bohnke, B. Vuillemin, C. Gabrielli, M. Keddam, H. Perrot, H. Takenouti and R. Torresi, *Electrochim. Acta* **40** (1995) 2755.
[7] T. S. De Gromoboy and L. L. Shreir, *Electrochim. Acta* **11** (1996) 895.
[8] S. Bourkane, C. Gabrielli and M. Keddam, *Electrochim. Acta* **38** (1993) 1827.
[9] K. J. Vetter, H.-H. Strehblow, *Ber. Bunsenges Phys. Chem.* **74** (1970) 449.